Thermospin effects in parallel coupled double quantum dots in the presence of the Rashba spin–orbit interaction and Zeeman splitting*

Xue Hui-Jie(薛惠杰)[a)b)], Lü Tian-Quan(吕天全)[a)†], Zhang Hong-Chen(张红晨)[c)], Yin Hai-Tao(尹海涛)[b)], Cui Lian(催 莲)[a)], and He Ze-Long(贺泽龙)[a)]

[a)] *Department of physics, Center for Condensed Matter Science and Technology, Harbin Institute of Technology, Harbin* 150001, *China*

[b)] *Heilongjiang Key Laboratory for Low Dimensional and Mesoscopic Physics, School of Physics and Electronic Engineering, Harbin Normal University, Harbin* 150025, *China*

[c)] *Space Materials and Environment Engineering Laboratory, Harbin Institute of Technology, Harbin* 150001, *China*

(Received 18 April 2011; revised manuscript received 9 October 2011)

The thermoelectric and the thermospin transport properties, including electrical conductivity, Seebeck coefficient, thermal conductivity, and thermoelectric figure of merit, of a parallel coupled double-quantum-dot Aharonov–Bohm interferometer are investigated by means of the Green function technique. The periodic Anderson model is used to describe the quantum dot system, the Rashba spin–orbit interaction and the Zeeman splitting under a magnetic field are considered. The theoretical results show the constructive contribution of the Rashba effect and the influence of the magnetic field on the thermospin effects. We also show theoretically that material with a high figure of merit can be obtained by tuning the Zeeman splitting energy only.

Keywords: thermospin effect, spin Seebeck coefficient, Zeeman splitting, Rashba spin–orbit interaction

PACS: 72.25.Dc, 73.21.La, 72.20.Pa **DOI:** 10.1088/1674-1056/21/3/037201

1. Introduction

The thermoelectric (TE) energy conversion technology is a feasible energy conversion technology, by which thermal energy can be converted into electrical energy directly. The TE material is a very useful functional material. The efficiency of the TE material is estimated by the dimensionless TE figure of merit (FOM) ZT, where T is the operating temperature of the device and $ZT = GS^2T/\kappa$. In order to obtain a high ZT value, electrical conductivity G and Seebeck coefficient S need to be increased, while thermal conductivity κ needs to be reduced. For the bulk material, ZT is restricted by the classical relationships of the coefficients, such as the Mott relation (an increase in the electrical conductivity leads to a decrease in the Seebeck coefficient)[1] and the Wiedemann–Franz law (the Lorentz ratio is $L = \kappa/GT = (k_B\pi)^2/3e^2$ for the bulk material, which means that an increase in the electrical conductivity leads to an increase in the thermal conductivity).[2] Those relations may not hold[3] due to the quantum phenomena and the Coulomb blockade effects emerging in nanostructure materials, which makes it possible to enhance ZT by modulating coefficients G, S, and κ simultaneously. In 1993, Hicks and Dresselhaus[4] first presented an idea that uses the low-dimensional structure materials to obtain a high FOM. The theoretical result shows that the FOM of the low-dimensional material is much larger than that of the bulk material. Hence, the nanostructure materials largely promote the development of the TE materials. With the development of the nanostructure fabricating technique, lots of work has been done on the TE transport properties of mesoscopic devices, such as quantum wires,[5] supperlattices,[6,7] and quantum dot systems.[8,9] However, the commercial applications of the nanostructure TE materials are restricted due to the complexity and the cost of the nanomaterials. Zero-dimensional systems, such as a single quantum dot[10] and a series of two quantum dots,[11] have been investigated as effective TE materials. The single quantum dot with a single en-

*Project supported by the Natural Science Foundation of Heilongjiang Province, China (Grant No. F200939).

†Corresponding author. E-mail: ltq@hit.edu.cn

© 2012 Chinese Physical Society and IOP Publishing Ltd

ergy level and that with multiple energy levels[12,13] have been investigated. Sánchez and Büttiker[14] have investigated the energy and current conversion mechanism for the quantum dots in a two-terminal device and drew the conclusion that the ratio of the charge current to the heat current is determined by the ratio of the charge quantum to the energy quantum. The directions of the energy flow and the charge motion are decoupled by using the master equation approach. The charge quantum and the energy quantum are very important for investigating the thermoelectric conversion of the two-terminal device.

The temperature gradient can also be used to generate the spin current. The spin-resolved phenomenon is called the thermospin effect or the spin dependent Seebeck effect. Since Uchida *et al.*[15] reported the spin dependent Seebeck effect in a ferromagnetic metal $Ni_{81}Fe_{19}$, this phenomenon has attracted much attention as a new method for generating spin currents from the heat energy. It opens up new possibilities for spintronic devices and a door for designing and fabricating thermospin quantum devices to generate spin currents by using the temperature gradient rather than the usual electric bias. Experiments on magnetic insulators and magnetic semiconductors show that the spin dependent Seebeck effect is conceptually different from the traditional thermoelectric effect, launching new challenges for both theorists and experimentalists.[16] Although there still exists some argument about the transportation of the spin in the material, lots of theoretical work has been done on the thermospin effect. Especially, the thermospin effect has been theoretically investigated in the low-dimensional quantum systems, such as the quantum wires[17−20] and a single quantum dot (QD) connected to the ferromagnetic leads in the presence of the Rashba spin–orbit interaction (RSOI) or the Zeeman field.[21,22] The thermospin effect of the double-coupled-quantum-dot molecule system has been investigated by Liu and Yang,[23] and they found that a pure spin-up (spin-down) Seebeck coefficient can be generated by the co-action of the magnetic flux and the RSOI at room temperature.[24] The RSOI and the temperature gradient are very important for spintronic applications. Motivated by this, we pay our attention to investigate the double-quantum-dot (DQD) system. The thermospin effect in the parallel coupled DQD in the presence of interdot coupling and Coulomb interactions has never been investigated, although it is an important structure for TE transport[25] and spin-dependent TE transport.[26]

We study the TE and the thermospin effects taking into account the RSOI and the Zeeman effects in the parallel coupled DQD. This kind of QD ring has been realized experimentally by using the droplet epitaxy technique.[27,28] For simplicity, we assume the transmission through the tunnel barriers to be sufficiently small so that the transport is defined by sequential tunneling of single electrons.[14] In the present work, a positive direction uniform magnetic field is added to a system containing QDs and a quantum ring. The interplay of the RSOI and the Zeeman splitting greatly influence the TE and the thermospin effects in the system. The pure spin Seebeck coefficient and a high FOM can be obtained.

2. Model and formulation

When an electric field and a magnetic field are applied to a system of charge and spin, there are four actions, i.e. the electric (or the Coulomb) force on the charge; the Lorentz force on the moving charge; the magnetic force on the spin (Zeeman); and the electric force on the moving spin induced by the relativistic effect (RSOI).[31] The magnetic field can cause intra level spin flip and provide the Zeeman energy that relieves the spin degeneracy. The magnetic field can also induce a spin polarization in an isolated QD. The spin polarization can also be obtained by the RSOI.

We consider an interesting case that could be instructive to the device application. We assume that the energy level of the QD is spin dependent, which can be realized by applying a magnetic field. The Hamiltonian of the system (see Fig. 1) contains the kinetic and the potential energies, the Zeeman energy, and the RSOI. We assume that the RSOI exists only in the QDs, and the arms of the ring and the leads are free of this interaction. The Hamiltonian reads

$$\begin{aligned} H =& \sum_{i,\sigma} (\varepsilon_i + \sigma\Delta B) d_{i\sigma}^{+} d_{i\sigma} \\ &+ \sum_{k,\sigma} \varepsilon_{\boldsymbol{k}\alpha} c_{\boldsymbol{k}\alpha\sigma}^{+} c_{\boldsymbol{k}\alpha\sigma} + \sum_{i} U_i \hat{n}_{i\uparrow} \hat{n}_{i\downarrow} \\ &+ \sum_{\boldsymbol{k}\alpha i\sigma} t_{\alpha i\sigma} (c_{\boldsymbol{k}\alpha\sigma}^{+} d_{i\sigma} + d_{i\sigma}^{+} c_{\boldsymbol{k}\alpha\sigma}) \\ &- t_{\mathrm{c}} \sum_{\sigma} (d_{1\sigma}^{+} d_{2\sigma} + d_{2\sigma}^{+} d_{1\sigma}), \end{aligned} \tag{1}$$

where $\varepsilon_{i\sigma} = \varepsilon_i + \sigma\Delta B$ is the spin dependent energy level for the QD, ε_i is the energy level in the dot, ΔB is the energy shift caused by the Zeeman splitting,

$\sigma = \pm 1$ ($\uparrow\downarrow$) represents the spin orientation, $d^+_{i\sigma}(d_{i\sigma})$ is the creation (annihilates) operator for the electron in the i-th dot with spin σ, $c^+_{\boldsymbol{k}\alpha\sigma}(c_{\boldsymbol{k}\alpha\sigma})$ is the creation (annihilation) operator of the electron in the lead with momentum $\boldsymbol{k}$, spin σ, and energy $\varepsilon_{\boldsymbol{k}\alpha}$. The electron–electron (e–e) interaction in the leads has been neglected. The second term on the right-hand side is the electron energy in the α (= L, R) lead. The third term is the Coulomb interaction between two electrons in the same dot with a constant strength U_i. The inter-dot electron interaction is ignored, since it is usually much smaller than the intra-dot interaction due to the screening effect. The forth term is the tunnel coupling of electron between the leads and the QDs with coupling strength $t_{\alpha i\sigma}$. The last term is the tunnel coupling between the QDs, and $t_{\rm c}$ is the inter-dot tunnel coupling strength.

The hopping matrix elements $t_{\alpha i\sigma}$ can be written as

$$\begin{aligned} t_{\rm L1\sigma} &= |t_{\rm L1}|\ {\rm e}^{{\rm i}\,\varphi/4}\,{\rm e}^{-{\rm i}\,\sigma\phi_{\rm R1}/2}, \\ t_{\rm R1\sigma} &= |t_{\rm R1}|\ {\rm e}^{-{\rm i}\,\varphi/4}\,{\rm e}^{{\rm i}\,\sigma\ \phi_{\rm R1}/2}, \\ t_{\rm L2\sigma} &= |t_{\rm L2}|\ {\rm e}^{-{\rm i}\,\varphi/4}\,{\rm e}^{-{\rm i}\,\sigma\phi_{\rm R2}/2}, \\ t_{\rm R2\sigma} &= |t_{\rm R2}|\ {\rm e}^{{\rm i}\,\varphi/4}\,{\rm e}^{{\rm i}\,\sigma\phi_{\rm R2}/2}, \end{aligned} \tag{2}$$

where $\varphi = 2\pi\Phi/\Phi_0$ is the phase shift due to the magnetic flux threading through the AB ring, $\Phi_0 = h/c$ is the flux quantum, $\varphi_{{\rm R}i}$ is the phase factor that arises from the RSOI in dot i,[31] and is related to the structure parameters by $\varphi_{{\rm R}i} = \alpha L_i m^*/\hbar^2$, α is the RSOI strength, L_i is the length of dot i, m^* is the electron effective mass.

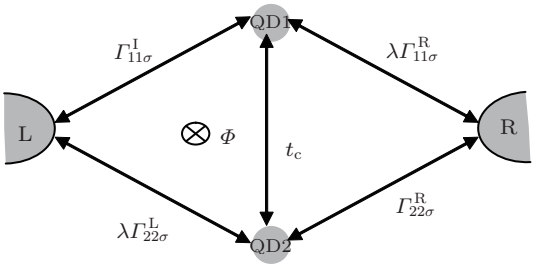


Fig. 1. Schematic diagram of the system under consideration. The two QDs are inserted into each arm of the ring and are mutually coupled through a tunnel junction with coupling strength $t_{\rm c}$. The electrons in the QDs interact with each other via the intra-dot Coulomb interaction. Both the intra-dot Coulomb interaction and the dot's energy level can be tuned by the gates and the tunnel junctions.[29] The quantum ring is connected to the outer environment by the left and the right leads. In addition, a magnetic flux (Φ) threads through the quantum ring.[30]

In the following calculation, we define the linewidth matrix elements as

$$\Gamma^{\alpha}_{ij\sigma} = 2\pi \sum_{\boldsymbol{k}} t_{\alpha i\sigma} t^*_{\alpha j\sigma} \delta(\varepsilon - \varepsilon_{\boldsymbol{k}\alpha}),$$

and $\Gamma = \Gamma^{\rm L} + \Gamma^{\rm R}$. Matrix $\Gamma^{\rm L(R)}_{\sigma}$ is given by

$$\Gamma^{\rm L(R)}_{\sigma} = \begin{pmatrix} \Gamma^{\rm L(R)}_{11} & \sqrt{\Gamma^{\rm L(R)}_{11}\Gamma^{\rm L(R)}_{22}}\,{\rm e}^{\pm{\rm i}\,\phi_\sigma/2} \\ \sqrt{\Gamma^{\rm L(R)}_{11}\Gamma^{\rm L(R)}_{22}}\,{\rm e}^{\mp{\rm i}\,\phi_\sigma/2} & \Gamma^{\rm L(R)}_{22} \end{pmatrix}, \tag{3}$$

where $\Gamma^{\rm L(R)}_{ij}$ is the phase-independent part of $\Gamma^{\rm L(R)}_{ij\sigma}$. The spin-dependent phase factor is $\phi_\sigma = \varphi - \sigma\varphi_{\rm R}$ with $\varphi_{\rm R} = \varphi_{\rm R1} - \varphi_{\rm R2}$. It is obvious that ϕ_σ depends only on the difference between phase factors $\varphi_{\rm R1}$ and $\varphi_{\rm R2}$ induced by the RSOI. Then the RSOI is assumed to exist in only one of the two dots.

In order to describe the TE and the thermospin effects clearly, we recall some basic formulae. Let the differences in voltage and temperature between the two leads be denoted as ΔV and ΔT, respectively, then we have charge current

$$I = eL_0\Delta\mu + \frac{e}{T}L_1\Delta T, \tag{4}$$

and heat current

$$I_Q = -L_1\Delta\mu - \frac{1}{T}L_2\Delta T, \tag{5}$$

where $\Delta\mu = e\Delta V$. The dynamic coefficient L_n ($n = 0, 1, 2$) are defined as

$$L_n = -\frac{1}{h}\,{\rm Tr}\int {\rm d}\varepsilon(\varepsilon-\mu)^n T(\varepsilon)\frac{\partial f}{\partial\varepsilon}, \tag{6}$$

where $f(\varepsilon) = [\exp((\varepsilon-\mu_\alpha)/k_{\rm B}T)+1]^{-1}$ is the Fermi–Dirac distribution function, and $T(\varepsilon)$ is the transmission probability through the dots which is in the spin space. The spin dependent transmission probability can be written as $T_\sigma(\varepsilon) = {\rm Tr}[G^{\rm a}_\sigma(\varepsilon)\Gamma^{\rm R}_\sigma G^{\rm r}_\sigma(\varepsilon)\Gamma^{\rm L}_\sigma]$, where $G^{\rm r}_\sigma(G^{\rm a}_\sigma)$ is the retarded (advanced) Green's function of the QD.

Generally, the TE Seebeck coefficient is defined as the voltage drop induced by the temperature difference under the condition of vanishing charge current $I = 0$. In the linear response regime, the well-known

formula for the TE Seebeck coefficient is given by

$$S = -\frac{\Delta V}{\Delta T} = -\frac{1}{eT}\frac{L_1}{L_0}. \tag{7}$$

When the spin polarization occurs, the dynamic coefficient can be written as $L_n = \sum_\sigma L_{n\sigma}$, where $L_{n\sigma}$ is spin dependent. When the spin polarization is considered, we can calculate the TE Seebeck coefficient under the condition that both the spin and the charge currents ($I_\uparrow = I_\downarrow = 0$) vanish simultaneously.

The charge (spin) electrical conductivity, the charge Seebeck coefficient, the spin Seebeck coefficient, and the thermal conductivity are given by

$$G_{\mathrm{c(spin)}} = \frac{1}{2}(G_\uparrow \pm G_\downarrow) = \frac{e^2}{2}(L_{0\uparrow} \pm L_{0\downarrow}), \tag{8}$$

$$S_{\mathrm{c}} = \frac{1}{2}(S_\uparrow + S_\downarrow) = -\frac{1}{2eT}\left(\frac{L_{1\uparrow}}{L_{0\uparrow}} + \frac{L_{1\downarrow}}{L_{0\downarrow}}\right), \tag{9}$$

$$\begin{aligned} S_{\mathrm{spin}} &= \frac{\Delta V_{\mathrm{spin}}}{\Delta T} = \frac{1}{2}(S_\uparrow - S_\downarrow) \\ &= -\frac{1}{2eT}\left(\frac{L_{1\uparrow}}{L_{0\uparrow}} - \frac{L_{1\downarrow}}{L_{0\downarrow}}\right), \end{aligned} \tag{10}$$

$$\kappa = \sum_\sigma \kappa_\sigma = \sum_\sigma \frac{1}{T}\left(L_{2\sigma} - \frac{L_{1\sigma}^2}{L_{0\sigma}}\right). \tag{11}$$

The FOM is given by

$$Z_{\mathrm{c(spin)}}T = \left|\frac{(2e/\hbar)G_{\mathrm{c(spin)}}S_{\mathrm{c(spin)}}^2 T}{\kappa}\right|. \tag{12}$$

The thermal conductivity can be written as $\kappa = \kappa_{\mathrm{ph}} + \kappa_{\mathrm{e}}$, where κ_{ph} is the lattice thermal conductivity. We assume that at low temperature, the lattice (phonon) thermal conductivity contribution can be neglected.

3. Numerical results and discussion

The tunneling coupling matrices between the dots and the leads are assumed to be $\Gamma_{11}^{\mathrm{L}} = \Gamma_{22}^{\mathrm{R}} = \Gamma$ and $\Gamma_{11}^{\mathrm{R}} = \Gamma_{22}^{\mathrm{L}} = \lambda\Gamma$ respectively, where λ is the structure parameter, which can change the structure from the serial configurationn ($\lambda = 0$) to the parallel configuration ($\lambda \neq 0$). In calculation, for simplicity, we take the unit of $\hbar = e = k_{\mathrm{B}} = 1$, Γ is used as the unit of energy, and the same bare energies of the QDs $\varepsilon_1 = \varepsilon_2 = \varepsilon_0 = 0$ are used. We fix $U_1 = U_2 = U$ and $t_{\mathrm{c}} = 1$ throughout this paper.

In this work, we focus on the influences of the quantum interference and the Zeeman effect on the thermospin effect of the DQD molecular junction. Once the transmission $T(\varepsilon)$ for the electron in the DQD system is known, the thermoelectric coefficient can be calculated straightforwardly. We first investigate the effects of the Zeeman splitting on the transmission spectra with parallel structure parameter $\lambda = 1$ and different values of intra-dot Coulomb interaction U, as shown in Fig. 2. In the case of $U = 0$, by using the molecular state representation, the coupling strengths of the bonding and the antibonding states with the leads can be determined by[32]

$$\Gamma_{\pm\sigma} = \Gamma \mp \Gamma\cos(\varphi_\sigma/2). \tag{13}$$

Around the bonding state, the transmission coefficient can be approximated by

$$T_{\mathrm{bonding},\sigma}(\varepsilon_{\mathrm{F}}) \approx \frac{1}{[(\varepsilon - \varepsilon_0 + t_{\mathrm{c}} - \sigma\Delta\mathrm{B})/\Gamma_{-\sigma}]^2 + 1}, \tag{14}$$

and around the antibonding state, the transmission coefficient is

$$\begin{aligned} &T_{\mathrm{antibonding},\sigma}(\varepsilon_{\mathrm{F}}) \\ &\approx T_\sigma \frac{[(\varepsilon - \varepsilon_0 - t_{\mathrm{c}} - \sigma\Delta\mathrm{B})/\Gamma_{+\sigma} + q_\sigma]^2}{[(\varepsilon - \varepsilon_0 - t_{\mathrm{c}} - \sigma\Delta\mathrm{B})/\Gamma_{+\sigma}]^2 + 1}, \end{aligned} \tag{15}$$

where $q_\sigma = -2t_{\mathrm{c}}/\Gamma_{-\sigma}$.

The magnitude of the effective coupling between the molecular states and the leads can be tuned by the strength of the RSOI and the magnetic flux. In the case of $\varphi_{\mathrm{R}} = \pi/4$ and $\varphi = \pi/2$, according to Eq. (13), the spin separation phenomena occur due to the different coupling strengths between the dots and the leads.[32] The quantum interference effects between the bonding and the antibonding states result in a Breit–Wigner resonance and a Fano resonance appearing in the spin-up electron linear transmission spectrum, as shown in Fig. 2(a). In the absence of Zeeman splitting, $\Delta B = 0$, the spin-up electron transmission of the Breit–Wigner resonance and the Fano resonance centered at the bonding state occurs at $\varepsilon_0 - t_{\mathrm{c}}$, and it occurs at $\varepsilon_0 + t_{\mathrm{c}}$ for that centered at the antibonding state. Due to the existence of the Zeeman splitting ΔB and the interdot tunnel coupling t_{c}, there are a total of four molecular states appearing in the double coupled QD molecular junction, and their energies are centered approximately at $\varepsilon_0 - t_{\mathrm{c}} - \Delta B$, $\varepsilon_0 - t_{\mathrm{c}} + \Delta B$, $\varepsilon_0 + t_{\mathrm{c}} - \Delta B$, and $\varepsilon_0 + t_{\mathrm{c}} + \Delta B$ corresponding to the corrections of the Zeeman splitting energy to the bonding and the antibonding molecular states. The positions of the resonance peaks are modulated by

tuning the Zeeman field. For a further increase of ΔB, the spin-up Breit–Wigner resonance and the Fano resonance keep shifting toward the positive-energy side, while the spin-down electron peak shifts toward the negative-energy side. The many-body effect is considered in Fig. 2(b), and the Fano peaks are divided into two groups, because the Coulomb repulsion splits the electron eigenenergy spectrum. A similar behavior to that in Fig. 2(a) appears with the increase of ΔB. The resonance energy levels locate at the energies of the bonding state, the antibonding state, and their Coulomb counterparts, i.e., $\varepsilon_0 \pm t_c \pm \Delta B$ and $\varepsilon_0 \pm t_c \pm \Delta B + U$. The spin-down electron transmission spectra have the opposite behaviors with the increase of ΔB, as shown in Fig. 2(b2).

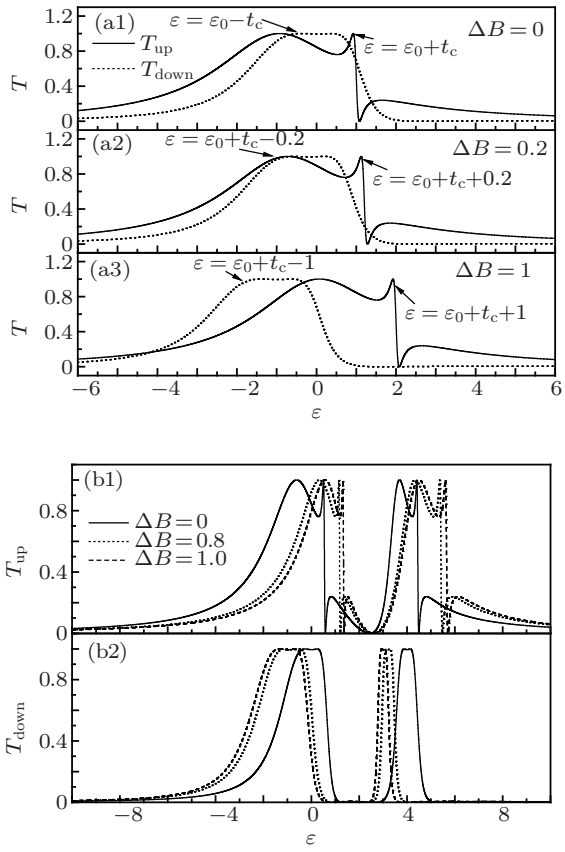


Fig. 2. Spin-dependent transmission coefficients as functions of Fermi energy ε for (a) $U=0$ and (b) $U=4$ with different values of ΔB, and $\varphi_R=\pi/4$, $\lambda=1$, $\varphi=\pi/2$.

In order to investigate the effect of the magnetic field on the DQD molecular junction, the spin-dependent TE coefficient and the spin Seebeck coefficient versus the Zeeman splitting ΔB are shown in Fig. 3. As mentioned above, with the increase of the Zeeman splitting ΔB, the two spin-up resonance centers shift toward the higher energy. Thus, the transmission probability at the Fermi energy first increases and then decreases with the increase of ΔB, which results in the spin-up transmission probability departing from the unitary limit. The Fano resonance located at the antibonding state becomes less important for the electron transmission at the Fermi level due to its increased distance away from the Fermi level. With the increase of the Zeeman splitting ΔB, the Breit–Wigner resonance passes through the Fermi level, this explains why the spin-up electrical conductance decreases. The spin-down electron transmission is different from the spin-up one. The behavior of the spin-up electron transmission varying with the Zeeman splitting is similar to that with the increase of the dot level in the device, while the spin-down electron has the opposite behavior to that with the increase of the dot level, since the spin-up and the spin-down electrons experience different potentials in the magnetic field. As a result, the conductance decreases with the increase of ΔB. The spin-up electron conductance first increases, and then decreases. While the spin-down electrical conductance first decreases, then increases, and then decreases again until the resonance is less important at the Fermi energy (see Figs. 2(b2) and 3(a)). Figure 3(b) shows that the spin-up Seebeck coefficient oscillates with ΔB smoothly. The Fermi energy has an important effect on the Seebeck coefficient (see Figs. 2(b1) and 3(b)). While the spin-down Seebeck coefficient oscillates with ΔB rapidly, the peaks become higher, which make the spin Seebeck coefficient oscillate with ΔB and change sign at the chemical potential sweeped by the DQD molecular states.

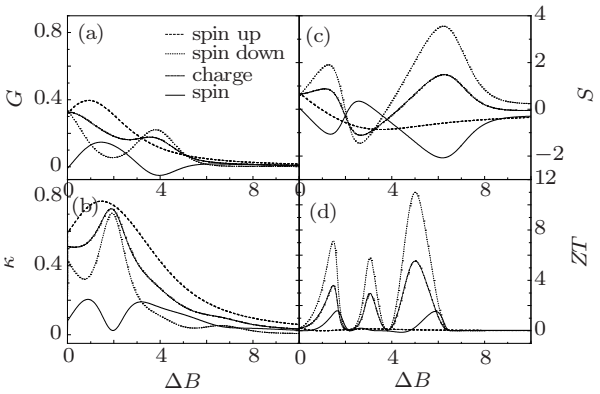


Fig. 3. Spin-dependent TE coefficients (a) G, (b) S, (c) k, and (d) ZT as functions of the Zeeman splitting with $\varphi_R=\pi/4$, $\varphi=\pi/2$, $T=0.5$, $\lambda=1$, and $U=4$.

The TE FOM is calculated and shown in Fig. 3(d). In the absence of ΔB, spin-up $ZT_\uparrow$ and spin-down $ZT_\downarrow$ are almost the same. A small difference is due to the RSOI and the magnetic flux in the

AB ring. Under a relatively big Zeeman splitting, the ZT originates from the contribution of the spin-down electron, i.e., the spin-down electron plays an important role. The Zeeman splitting corrects the molecular states sweeping the chemical potential, the value of the charge FOM ZT exceeds 1, which indicates possible applications of the system to TE power generators or cooling systems.

The Seebeck coefficient is a sensitive tool to detect the TE conversion. The spin dependent transport is a hot topic in recent years.[33,34] The spin Seebeck coefficient can measure the ability to generate spin current in a spintronic device and is different from the charge Seebeck coefficient. Figure 4 shows spin Seebeck coefficient $S_{\rm S}$ versus $\varphi_{\rm R}$ for different values of ΔB. It can be seen that the curves are asymmetric due to the electron–hole symmetry.[12] In order to show clearly the varying characteristic of $S_{\rm S}$ with $\varphi_{\rm R}$, two-period curves are given. In the case of $\Delta B = 0$, when $\varphi_{\rm R} = 0$, $S_{\rm S} = 0$, because the spin polarization is absent at the absence of the RSOI, i.e., $S_\uparrow = S_\downarrow$. With the increase of $\varphi_{\rm R}$, since the spin-up and the spin-down electrons have different phase factors, the spin-up and the spin-down Seebeck coefficients become different from each other, then $S_\uparrow \neq S_\downarrow$, and $S_{\rm S}$ is thus introduced to the DQD molecular junction. With a fixing ΔB, it is interesting that $S_{\rm S}$ oscillates with $\varphi_{\rm R}$ periodically and the sign reverses regularly at each 2π interval. When the RSOI induces phase $\varphi_{\rm R} = (2n+1)\pi$, the spin Seebeck coefficient reaches the maximum or the minimum, and $S_{\rm Smax} = -S_{\rm Smin}$ in the whole period, associated with Fano line-shape transmission spectra. With the increase of the Zeeman splitting ΔB, the sign reversal of $S_{\rm S}$ occurs, the curve shifts downward, and small peaks and valleys appear at the two sides of $\varphi_{\rm R} = (2n+1)\pi$, $(n = 0, 1, 2, \ldots)$. Combining Eq. (10) with our figure, we can conclude that the pure spin-up or spin-down Seebeck coefficient can be obtained in a certain RSOI strength in the presence of the Zeeman splitting, which can provide a new way to control the spin polarization in the spin devices. It is noted that there are three features in Fig. 4 for the corresponding $S_{\rm S}$. (i) The sign of $S_{\rm S}$ changes with the enhancement of the Zeeman splitting, i.e, the molecular state sweeping the chemical potential makes the sign reversal of the spin Seebeck coefficient associated with the Fano line shapes in the transmission spectrum. (ii) The value of $S_{\rm S}$ is enhanced obviously at $\varphi_{\rm R} = (2n+1)\pi$. (iii) The pure spin Seebeck coefficient can be obtained by tuning the Zeeman splitting. Our results indicate that the DQD molecular junction may be used as a better spintronic device.

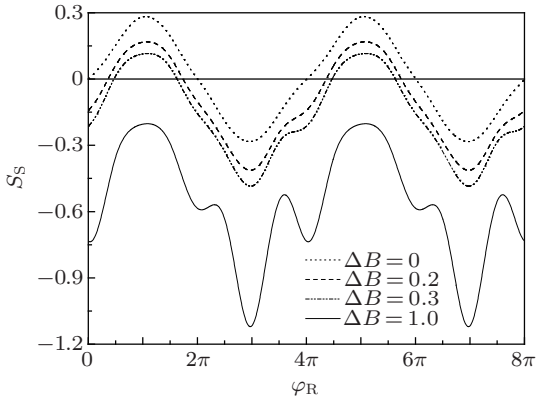


Fig. 4. Spin Seebeck coefficient $S_{\rm S}$ versus $\varphi_{\rm R}$ with $\varphi = \pi/2$, $T = 0.5$, $\lambda = 1$, $U = 4$, and different values of Zeeman splitting energy ΔB.

The phase coherence enables us to investigate the effects of the Aharonov–Bohm (AB) oscillation as well as the Fano interference on the TE properties.[8,9] The spin Seebeck coefficient $S_{\rm S}$ versus temperature T is described in Fig. 5(a). The curves indicate that the spin Seebeck coefficient is very sensitive not only to the Zeeman splitting field but also to the magnetic flux through the AB ring. In Fig. 5(a), we assume that the magnetic flux in the AB ring does not exist, the Zeeman splitting is zero ($\Delta B = 0$), and the spin Seebeck coefficient is zero. It is due to the spin-unpolarized phenomenon in the absence of magnetic field.[28] As for $\Delta B = 1$, in the case of $T < 0.07\Gamma$, the sign is positive. But for $0.07\Gamma < T < 10\Gamma$, the sign is negative. In the presence of magnetic flux (Fig. 5(b)), the sign of the spin Seebeck coefficient is almost negative in the whole temperature range. The RSOI and the magnetic field influence the efficiency of heat-electricity conversion remarkably, which is described in general by the dimensionless FOM. Figure 5(c) shows the dependence of spin FOM on temperature. It can be found that when a magnetic flux threads through the AB ring, the spin FOM exceeds 1 in the case of $\Delta B = 1$. The heat and electric convert efficiency is higher than that in the absence of magnetic flux. It has a similar behavior to that in Fig. 3, in which for the spin-up case, the FOM is zero in the whole range of temperature, and the spin-down one contributes to the FOM significantly. When temperature T is increased, the thermoelectric effect is enhanced obviously when the chemical potential is close to the energy of the molecular state.

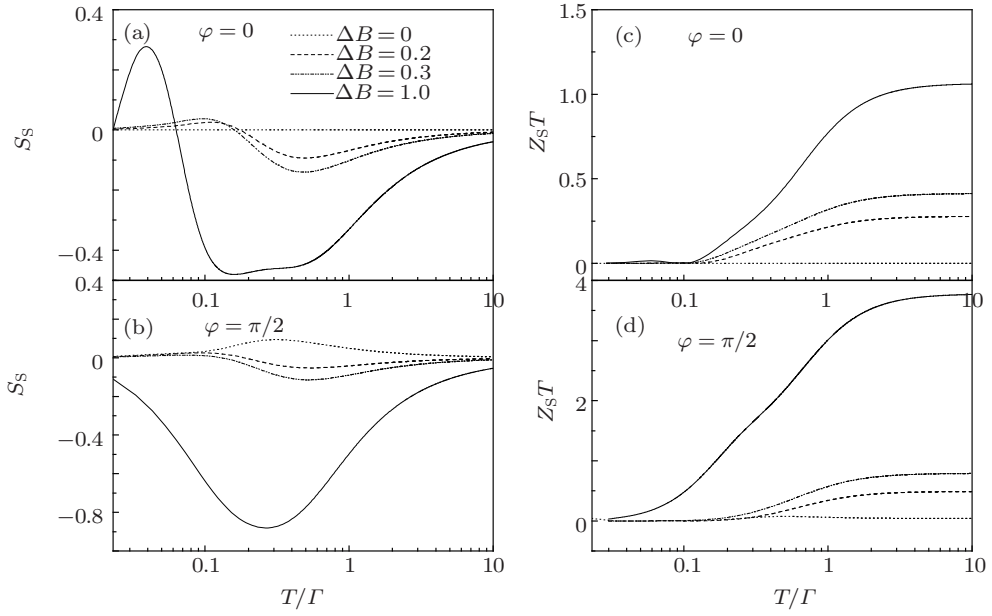


Fig. 5. Spin Seebeck efficient S_S ((a) and (b)) and spin FOM $Z_S T$ ((c) and (d)) versus temperature T at different values of ΔB and magnetic field flux ϕ for $\varphi_R = \pi/4$, $\lambda = 1$, and $U = 4$.

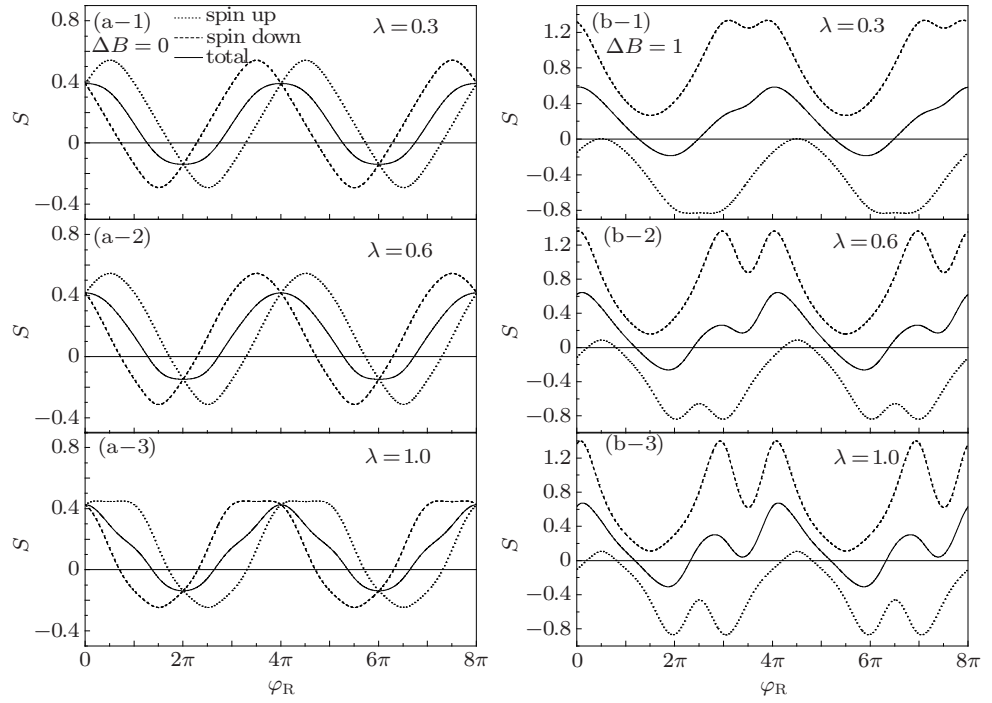


Fig. 6. Spin-dependent and charge Seebeck coefficients versus the Rashba spin–orbit interaction induced phase φ_R with different asymmetric coupling strengths between dots and leads for (a) $\Delta B = 0$ and (b) $\Delta B = 1$.

Varying structural parameter λ in our model, we also study how the value of λ influences the TE and the thermospin effects. In this paper, the parallel coupled DQD system with structural parameter $\lambda \neq 0$ is our topic. Figure 6(a) indicates that in the absence of the Zeeman splitting ΔB, the structural parameters have little effect on the spin-dependent Seebeck coefficient. Figure 6(b) shows that in the presence of the Zeeman splitting ΔB, the spin-down Seebeck coefficient reaches the maxima at the sides of 0, 3π, and 4π respectively, and the sign does not change in the whole period, corresponding to the hole-like transport. While the spin-up Seebeck coefficient valleys are present at $\varphi_R = 2\pi$ and 3π respectively, and the

spin-up Seebeck coefficient sign reversal occurs with the increase of λ. The curves for the spin-dependent TE Seebeck coefficient present more peaks with the increase of the Zeeman splitting energy ΔB. Thus, adjusting the structural parameters and the Zeeman splitting energy, the expected spin-up and spin-down TE Seebeck coefficients can be obtained.

4. Conclusion

The TE and the thermospin effects in the parallel DQD system in correlation with the RSOI and the Zeeman splitting are investigated by using the Green function technique. The results show that the co-actions of the RSOI, the magnetic flux, and the Zeeman splitting can help us control the type of the TE material (N-type or P-type) of the QD system, to generate the pure spin Seebeck coefficient, and to enhance the heat and electron conversion efficiency in the parallel coupled DQD system.

References

[1] Cutler M and Mott N F 1969 *Phys. Rev.* **181** 1336
[2] Snyder G J and Toberer E S 2008 *Nat. Mater.* **7** 105
[3] Kubala B, König J and Pekola J 2008 *Phys. Rev. Lett.* **100** 066801
[4] Hicks L D and Dresselhaus M S 1993 *Phys. Rev.* B **47** 16631
[5] Blanter Y M, Bruder C, Fazio R and Schoeller H 1997 *Phys. Rev.* B **55** 4069
[6] Lin C P J and Reinecke T L 1995 *Phys. Rev.* B **51** 13244
[7] Humphrey T E and Linke H 2005 *Phys. Rev. Lett.* **94** 096601
[8] Kim T S and Hershfield S 2002 *Phys. Rev. Lett.* **88** 136601
[9] Kim T S and Hershfield S 2003 *Phys. Rev.* B **67** 165313
[10] Swirkowicz R, Wierzbicki M and Barnas J 2009 *Phys. Rev.* B **80** 195409
[11] Chi F, Zheng J, Lu X D and Zhang K C 2011 *Phys. Lett.* A **375** 1352
[12] Liu J, Sun Q F and Xie X C 2010 *Phys. Rev.* B **81** 245323
[13] Swirkowicz R and Wierzbicki M 2010 *Phys. Rev.* B **82** 165334
[14] Sánchez R and Büttiker M 2011 *Phys. Rev.* B **83** 085428
[15] Uchida K, Takahashi S, Harii K, Ieda J, Koshibae W, Ando K, Maekawa S and Saitoh E 2008 *Nature* **455** 778
[16] Sinova J 2010 *Nat. Mater.* **9** 880
[17] Li Y X and Li B Z 2004 *Phys. Lett.* A **330** 274
[18] Li Y X and Li B Z 2005 *Chin. Phys.* **14** 1009
[19] Li Y X 2006 *Phy. Lett.* A **358** 70
[20] Lü H F, Zhu L C, Zu X T and Zhang H W 2010 *Appl. Phys. Lett.* **96** 12311
[21] Swirkowicz R, Wierzbicki M and Barnas J 2009 *Phys. Rev.* B **80** 195409
[22] Zhu L C, Jiang X D, Zu X T and Lü H F 2010 *Phys. Lett.* A **374** 4269
[23] Liu Y S and Yang X F 2010 *J. Appl. Phys.* **108** 023710
[24] Liu Y S, Chi F, Yang X F and Feng J F 2011 *J. Appl. Phys.* **109** 053712
[25] Liu Y S, Zhang D B, Yang X F and Feng J F 2011 *Nanotechnology* **22** 225201
[26] Xue H J, Lü T Q, Zhang H C, Yin H T, Cui L and He Z L 2011 *Chin. Phys.* B **20** 027301
[27] Liang L, Wang Z M, Lee J H, Mazur Y I, Shih C K and Salamo G J 2008 *ACS Nano* **2** 2219
[28] Chi F and Li S S 2006 *J. Appl. Phys.* **99** 043705
[29] Van der Wiel W G, Franceschi S D, Elzerman J M, Fujisawa T, Tarucha S and Kouwenhoven L P 2003 *Rev. Mod. Phys.* **75** 1
[30] Chi F and Zhao H L 2010 *Superlattices and Mirostructures* **47** 452
[31] Sun Q F, Wang J and Guo H 2005 *Phys. Rev.* B **71** 165310
[32] Yin H T, Lü T Q, Sun P N, Liu X J and Xue H J 2009 *Phys. Lett.* A **373** 3085
[33] Yin H T, Lü T Q, Liu X J and Xue H J 2010 *Phys. Status. Solidi.* B **247** 150
[34] Huang R, Wu S Q and Yan C H 2010 *Chin. Phys.* B **19** 077302
[35] Wang R, Kong L M, Zhou Y Q, Zhang C X and Xing Z Y 2010 *Chin. Phys.* B **19** 127202